Title	Caustic graphene plasmons with Kelvin angle
Author(s)	Shi, Xihang; Lin, Xiao; Gao, Fei; Xu, Hongyi; Yang, Zhaoju; Zhang, Baile
Citation	Shi, X., Lin, X., Gao, F., Xu, H., Yang, Z., & Zhang, B. (2015). Caustic graphene plasmons with Kelvin angle. Physical Review B, 92, 081404(R)-.
Date	2015
URL	http://hdl.handle.net/10220/39142
Rights	

Caustic graphene plasmons with Kelvin angle

Xihang Shi,[1] Xiao Lin,[1] Fei Gao,[1] Hongyi Xu,[1] Zhaoju Yang,[1] and Baile Zhang[1,2,*]

[1]*Division of Physics and Applied Physics, School of Physical and Mathematical Sciences, Nanyang Technological University,*
Singapore 637371, Singapore
[2]*Centre for Disruptive Photonic Technologies, Nanyang Technological University, Singapore 637371, Singapore*

A century-long argument made by Lord Kelvin that all swimming objects have an effective Mach number of 3, corresponding to a Kelvin angle of 19.5° for ship waves, has been challenged recently with the conclusion that the Kelvin angle should gradually transit to the Mach angle as the ship's velocity increases. Here we show that a similar phenomenon can happen for graphene plasmons. By analyzing the caustic wave pattern of graphene plasmons stimulated by a swift charged particle moving uniformly above graphene, we show that at low velocities of the charged particle, the caustics of graphene plasmons form the Kelvin angle. At large velocities of the particle, the caustics disappear and the effective semiangle of the wave pattern approaches the Mach angle. Our study introduces caustic wave theory to the field of graphene plasmonics, and reveals a physical picture of graphene plasmon excitation during electron energy-loss spectroscopy measurements.

Graphene plasmons [1–5], as typical two-dimensional (2D) plasmons confined on a 2D surface [6], have recently emerged as a new research branch in photonics that has attracted substantial research efforts. A typical quantitative measurement on graphene plasmons relies on the electron energy-loss spectroscopy (EELS) measurement [7–10]. In studying planar surfaces with EELS, a particularly instructive situation is when the electron is directed parallel to the surface [11]. This configuration has been extensively studied for other materials both experimentally and theoretically before the discovery of graphene [12–19], and recently has also been studied for graphene [20–22]. The unique dispersion of graphene plasmons compared to surface plasmons at a metal/dielectric interface may cause interesting phenomena that have yet to be revealed.

The fact that 2D plasmons, including graphene plasmons, exhibit a dispersion that is similar to that of deep-water waves in the long wavelength limit, has already been known for more than 50 years [1,5,6,23]. This implies that many deep-water-wave phenomena can find counterparts in graphene plasmons. Recently, a century-long celebrated prediction made by Lord Kelvin in the 1880's that the semiangle of ship waves on the water surface is fixed at 19.5°, independent of the ship's velocity [24,25], has been challenged by the conclusion that the ship-wave semiangle should gradually transit from a Kelvin angle to a Mach angle as the ship's velocity increases [26,27]. Kelvin made his prediction based on the dispersion of deep-water waves, while the recent studies argued that the deep-water waves excited by a ship should have preferred directions determined by the Frouder number, or the velocity of the ship, given a fixed ship size.

Note that the recently explored plasmonic Cherenkov radiation, which is similarly excited by a swift electromagnetic source moving on semiconductor surfaces [19] and metal surfaces [28], being analogous to traditional Cherenkov radiation, is fundamentally different from Kelvin ship waves. In plasmonic Cherenkov radiation, similar to traditional Cherenkov radiation, the Cherenkov angle (i.e., the semiangle of the Cherenkov cone) is a variable depending on the velocity of the source. That is why the Cherenkov angle is measured in high energy physics to characterize the speed of charged particles. However, the Kelvin angle for Kelvin ship waves is a fixed number of 19.5°, irrelevant to the speed of the ship from Kelvin's viewpoint.

In this Rapid Communication, we adopt the approaches of caustic wave theory to analyze graphene plasmons excited by a swift charged particle moving above the graphene plane. Previously, caustics have been treated predominantly on the level as envelopes of families of rays [29]. Recently, they have been used to generate arbitrary bending surface plasmon beams [30] on a metal surface, and discussed in the scattering of electron flow from graphene *p-n* junctions [31,32]. Yet caustics have not been discussed in the context of graphene plasmons. Here we study the wave aspects of caustics formed by graphene plasmons when a swift charged particle is moving parallel to the graphene plane. We find that at a relatively small velocity (∼0.1*c* or smaller, where *c* is the velocity of light in vacuum) of the swift charged particle, the stimulated graphene plasmons are confined within the nonsingular caustic boundaries with a semiangle of 19.5°, i.e., the Kelvin angle. These caustic boundaries are associated with cusp wave fronts and thus can be classified as fold caustics [29]. Each point within the caustic boundaries is covered twice by rays, whereas outside there is no ray. The more exact calculation with the Airy integral distinguishes the caustic shadow from the caustic zone, thus providing a complete wave description of caustic graphene plasmons. As the velocity of the charged particle increases, the graphene-plasmonic waves reaching the caustic boundaries become weak, which blurs the caustics and eventually makes them disappear. The calculation shows that the effective semiangle of the wave pattern approaches the Mach angle, which is similar to recent studies of ship waves in fluid mechanics.

We first introduce the calculation model, as illustrated in Fig. 1, where a particle with charge *q* moves along the $\hat{z}$ direction with a uniform velocity v parallel to an isolated graphene sheet at $y = d$. The current density that this charged
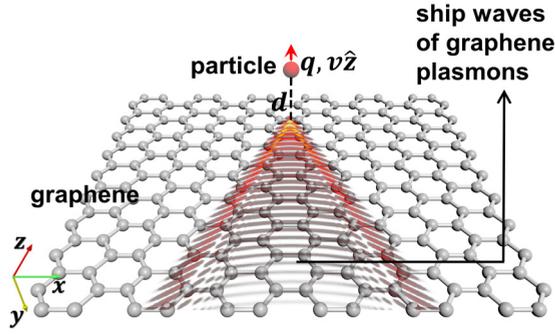
*blzhang@ntu.edu.sg

FIG. 1. (Color online) The ship waves of graphene plasmons excited by a charged particle moving along the z direction with constant velocity v. The distance between the graphene and the particle is d.

particle generates is

$$\mathbf{J}(\mathbf{r},t) = \hat{z}qv\delta(x)\delta(y)\delta(z - vt), \qquad (1)$$

and its Fourier transform is

$$\mathbf{J}(\mathbf{r},\omega) = \hat{z}\frac{q}{4\pi^2\rho}e^{i\omega z/v}\delta(\rho), \qquad (2)$$

where $\rho = \sqrt{x^2 + y^2}$. The evanescent fields from the swift charged particle can excite graphene plasmons on graphene. In the calculation we set $d = 1$ μm. The isolated graphene is assumed to have a chemical potential of $\mu_c = 0.15$ eV, and a scattering rate of $\Gamma = 0.11$ meV at room temperature $T = 300$ K [33]. The frequency dependent complex conductivity $\sigma(\omega)$ of the isolated graphene is computed from the Kubo formula [33,34]. Each frequency component of the graphene plasmons is exactly derived by taking the residue of the Sommerfeld pole [35–37]. The frequency components of excited graphene plasmons are mostly below 50 THz, above which the interband transition in graphene will dominate and cause a large loss [1,2,23]. After taking the residue of the Sommerfeld pole, we use the vertical component of electrical field E_y to represent the transverse-magnetic (TM) graphene plasmons,

$$E_y(\omega) = \frac{-iq}{4\pi v\varepsilon_0}\frac{k_y^2}{k_x}e^{ik_yd+ik_xx+ik_zz}, \qquad (3)$$

where $k_y = -2\omega\varepsilon_0/\sigma(\omega)$ indicates the confinement of graphene plasmons, $k_z = \omega/v$ and $k_x = \sqrt{\omega^2\varepsilon_0\mu_0 - k_y^2 - k_z^2}$ are the wave vectors of graphene plasmons, and ε_0 and μ_0 are the constitutive parameters of vacuum. The field distribution at time t is the Fourier integral of Eq. (3),

$$E_y(y = d,t) = 2\,\mathrm{Re}\left[\int \frac{-iq}{4\pi v\varepsilon_0}\frac{k_y^2}{k_x}e^{ik_yd}e^{ik_xx+ik_zz-i\omega t}d\omega\right]$$

$$= 2\,\mathrm{Re}\left[\int e_y(\omega)e^{ik_yd}e^{i\psi(\omega)t}d\omega\right], \qquad (4)$$

where $\psi(\omega) = k_x\frac{x}{t} + k_z\frac{z}{t} - \omega$ and $e_y(\omega) = \frac{-iq}{4\pi v\varepsilon_0}\frac{k_y^2}{k_x}$.

We then discuss the situation when the velocity of the particle is set to be $v = 0.1c$. We numerically carry out the integration in Eq. (4) to get the wave pattern, as shown in Fig. 2(a). The left part is the absolute value of the electrical
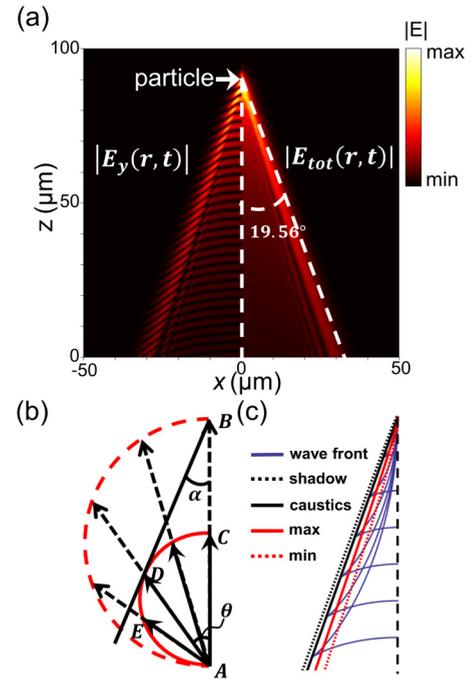

FIG. 2. (Color online) The ship wave of graphene plasmons excited by a swift charged particle with velocity $v = 0.1c$. (a) The absolute value of the electric field $|E_y(r,t)|$ (left) and the absolute value of the total electrical field $|E_{\mathrm{tot}}(r,t)|$ (right) of the wave pattern. The arrow indicates the position of the particle. (b) The Kelvin angle can be determined in a simple geometry. (c) The blue lines represent the wave fronts. The black dotted line is the boundary of the caustic shadow. The black solid line is the caustic boundary. The red line and the red dotted line are the maximum and minimum amplitudes in the neighborhood of the caustics.

field $|E_y(r,t)|$ and the right part is the absolute value of the total electrical field $|E_{\mathrm{tot}}(r,t)|$. The arrow indicates the position of the charged particle. The semiangle of 19.5°, i.e., the Kelvin angle, is clearly seen. A planelike wave is inside the wave pattern, following the charged particle.

An intuitive picture, following the approach of Kelvin [24,25], from the viewpoint of ray theory, is shown in Fig. 2(b). Consider the period when the particle moves from point A to point B with velocity v. The ship waves of graphene plasmons excited at point A will propagate in all directions with different frequencies. In the propagation direction of angle θ [as indicated in Fig. 2(b)], where $\cos\theta = k_z/\sqrt{k_x^2 + k_z^2}$, the phase velocity v_p of graphene plasmons must satisfy the stationary condition $v_p = v\cos\theta(\omega)$ [24,25]. When the particle arrives at point B, the dashed red circle represents the loci of all the arrived phases of the graphene plasmon waves. However, the group velocity v_g is only about half of the phase velocity v_p [37], thus the loci of the energy of the arrived waves form the solid red circle with the diameter only half of the red dashed one. The waves propagating in the direction $\theta = 35°$ form the Kelvin caustic boundary with angle $\alpha = \sin^{-1}(1/3) = 19.5°$, as shown by the solid black lines in Figs. 2(b) and 2(c). According to the ray tracing theory [37], the wave fronts are drawn as the blue lines in Fig. 2(c). All the wave fronts have cusps at the caustic boundary.

We can asymptotically evaluate the integral in Eq. (4) with the stationary phase method. The integration contour of Eq. (4) can be deformed in the complex ω plane and the only contribution comes from the path of steepest descent [24] around the stationary value $\omega = \omega_s$, where

$$\frac{d\psi(\omega)}{d\omega} = \frac{dk_x}{d\omega}\frac{x}{t} + \frac{dk_z}{d\omega}\frac{z}{t} - 1 = 0. \quad (5)$$

Equation (5) is equivalent to the group velocity concept in the ray tracing theory [37]. The expansion of ψ around ω_s is

$$\psi(\omega) = \psi(\omega_s) + \tfrac{1}{2}\psi''(\omega_s)(\omega - \omega_s)^2 + O(|\omega - \omega_s|^3). \quad (6)$$

Then the integral in Eq. (4) can be approximated as

$$E_y(y = d, t) = 2\mathrm{Re}\left[e_y(\omega_s)\frac{\sqrt{2\pi}}{\sqrt{\psi''(\omega_s)t}}e^{ik_y(\omega_s)d + i\psi(\omega_s)t + i\pi/4}\right]. \quad (7)$$

Equation (7) diverges when $\psi''(\omega) = 0$. In this case the path of steepest descent has to be chosen differently. It can be shown that for the frequency component $\omega = \omega_c$, where

$$\frac{d^2\psi(\omega)}{d\omega^2} = \frac{d^2k_x}{d\omega^2} = 0, \quad (8)$$

the first derivative of the group velocity with respect to frequency vanishes. Therefore the rays run together near such points, and the loci of such points form caustics or a caustic boundary, which separates a region without rays from another region covered twice by rays. We get the caustic boundary equation by combining Eqs. (5) and (8),

$$2\sqrt{2}\sqrt{1 - \left(\frac{v}{c}\right)^2}\frac{x}{vt} + \frac{z}{vt} = 1, \quad (9)$$

whose solution is shown by the black solid line in Fig. 2(c). When $v = 0.1c$, the exact angle of the caustics is $\alpha = 19.56°$.

To calculate the field around the caustics, we expand ψ around ω_c,

$$\psi(\omega) = \psi(\omega_c) + \psi'(\omega_c)(\omega - \omega_c) + \tfrac{1}{6}\psi'''(\omega_c)(\omega - \omega_c)^3 + O[(\omega - \omega_c)^4]. \quad (10)$$

In the neighborhood of the caustics, the first derivative of the phase [i.e., $\psi'(\omega_c)$] is almost, but not exactly, equal to zero. Substituting Eq. (10) into Eq. (4), the asymptotic form of $E_y(y, t)$ can be calculated with the Airy integral [37],

$$E_y(y = d, t) = 2\mathrm{Re}\left\{2\pi e_y(\omega_c)\left[\frac{t}{2}\psi'''(\omega_c)\right]^{-(1/3)} \times e^{ik_y(\omega_c)d + i\psi(\omega_c)t}\mathrm{Ai}(X)\right\}, \quad (11)$$

where $\mathrm{Ai}(X)$ is the Airy integral function and

$$X = \frac{t\psi'(\omega_c)}{[t\psi'''(\omega_c)/2]^{1/3}}. \quad (12)$$

When $X = 0$, Eq. (12) represents the caustic boundary. When $X > 0$, Eq. (12) represents the caustic shadow region, where, because of the Airy function, the field decays exponentially. When $X = 0.66$, the Airy function reaches $1/e$ of its maximum

(a)

$|E_y(r,t)|$ $|E_{tot}(r,t)|$
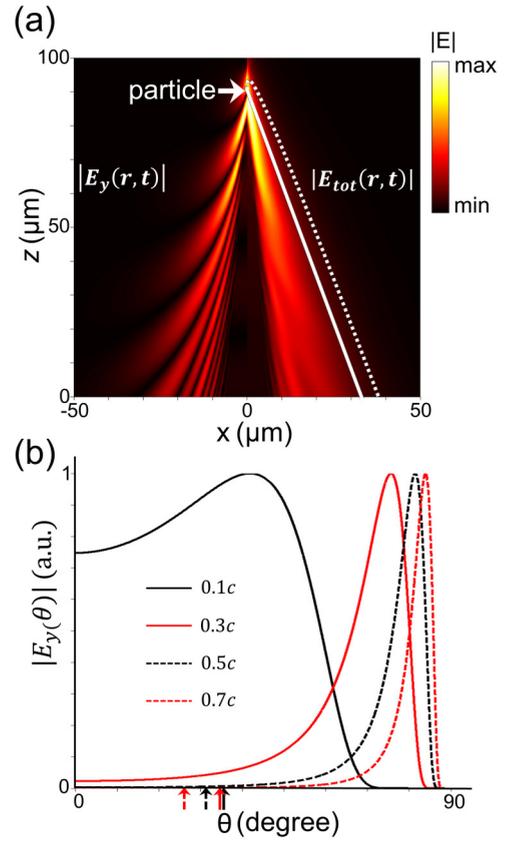
(b)

—— $0.1c$
—— $0.3c$
----- $0.5c$
----- $0.7c$

FIG. 3. (Color online) The ship waves of graphene plasmons excited by a swift charged particle with velocity $v = 0.3c$. (a) The electric field $|E_y(r,t)|$ (left) and the total electrical field $|E_{tot}(r,t)|$ (right) of the plasmonic ship waves. The arrow indicates the position of the particle. The white solid line represents the caustics and the white dotted line is the boundary of the caustic shadow. (b) The normalized distribution of $|E_y|$ over propagation angle θ. The velocity of the particle varies from $0.1c$, $0.3c$, $0.5c$, to $0.7c$. The arrows at the horizontal axis point to the angles at which the waves can reach the caustics.

value. We set $X = 0.66$ to represent the boundary of the caustic shadow, as shown by the dashed black line in Fig. 2(c). The Airy function reaches maximum at $X = -1.02$. The region between $X = 0$ and $X = -1.02$ corresponds to the caustic zone. The field in the caustic zone is relatively strong in the neighborhood of caustics as the wave-field focusing effect on caustics [29]. The field focusing in the caustic zone can be observed in Fig. 2(a) near the caustic boundary. The Airy function vanishes at $X = -2.34$. It means the field distribution has a minimum value, as shown by the dashed red line in Fig. 2(c). It can also be seen in Fig. 2(a) that a dark line (relatively weak field amplitude) separates the neighborhood of caustics from the waves confined by the two branches of caustics. The field amplitude in the neighborhood of the caustics decays more slowly, with $t^{-1/3}$ as shown by Eq. (11), than the field amplitude in the region inside the caustics, with $t^{-1/2}$ as shown by Eq. (7).

When the velocity of the charged particle is chosen to be $0.3c$, the wave pattern of graphene plasmons is shown in Fig. 3(a). The solid white line represents the caustic boundary

defined by Eq. (9). The dashed white line is the boundary of the caustic shadow defined by Eq. (12) with $X = 0.66$. Compared with Fig. 2(a), the angle between the caustic boundary and the z axis increases slightly and the caustic shadow expands, but the lightest branch of the waves contracts. Besides, there is no planelike wave at the center of the wave pattern.

To understand the transition of the wave pattern, we rewrite Eq. (4) as an integration over the propagation angle θ,

$$E_y(y = d, t) = 2\text{Re}\left[\int e_y e^{ik_y d} e^{i\psi(\omega)t} \frac{d\omega}{d\theta} d\theta\right]$$

$$= \text{Re}\left[\int E_y(\theta) e^{i\psi(\omega)t} d\theta\right], \quad (13)$$

where

$$E_y(\theta) = 2e_y e^{ik_y d} \frac{d\omega}{d\theta}. \quad (14)$$

The dependence of $|E_y(\theta)|$ on angle θ is shown in Fig. 3(b) with different velocities. When the velocity is $0.1c$, $|E_y(\theta)|$ has a relatively high value from $0°$ to $60°$. When the velocity increases to $0.3c$, $0.5c$, and $0.7c$, relatively high values of $|E_y(\theta)|$ occur at large propagation angles. The propagation angles at which the waves will reach the caustic boundary are $\theta = 35.1°, 34.0°, 31.5°$, and $26.8°$, corresponding to velocities of $0.1c$, $0.3c$, $0.5c$, and $0.7c$, respectively, as marked by the arrows in Fig. 3(b) at the horizontal axis. However, the wave amplitudes at these angles for velocities $0.3c$, $0.5c$, and $0.7c$ are so weak that they are difficult to perceive. Therefore, as the velocity increases from $0.1c$, the caustics get blurred and eventually disappear. At this moment, the effective boundary of the wave pattern is determined instead by the outermost perceivable fields.

As shown in Figs. 2(b) and 3(b), the outermost perceivable fields at large velocities of the particle are contributed by waves with a large propagation angle θ, corresponding to group velocity v'_g. It can be shown that as the particle's velocity v increases, v'_g tends to be independent of v [37]. Therefore, $\alpha \approx \frac{v'_g}{v} \propto 1/v$ and the effective semiangle of the wave pattern behaves as a Mack angle. The wave patterns of graphene plasmons excited by the swift charged particle with velocities $0.5c$ and $0.7c$ are shown in Figs. 4(a) and 4(b), respectively. Compared with Figs. 2(a) and 3(a), the wave patterns get more contracted as the velocity increases further. In Fig. 2(a), we find that in the horizontal line $z = 0$, the absolute of the total electrical field at the caustic point is 0.61 relative to its maximum value along the line. We use this as a criterion to determine the angle of the ship waves at different velocities of the charged particle, and the results are shown in Fig. 4(c). The angle of $\alpha = 19.47°$ is the angle of the caustic boundary at zero velocity limitation from Eq. (9). We plot the Mach angle line $\alpha = 4.52/v$ with the coefficient 4.52 adopted from the wave pattern when the particle's velocity is $0.9c$. The results show clearly the transition from the Kelvin angle of $19.5°$ at small velocities of the charged particle to the Mach angle at
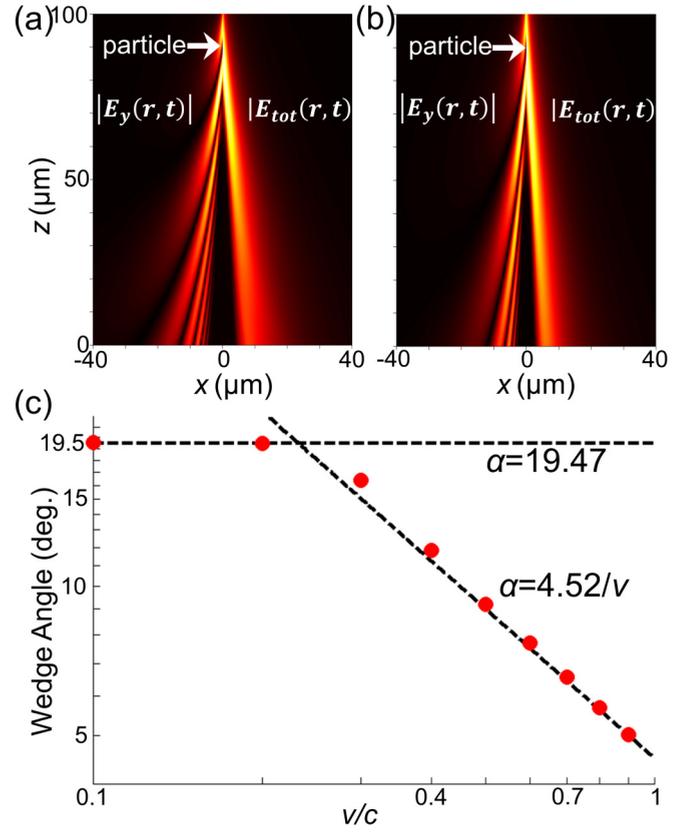

FIG. 4. (Color online) The ship waves of graphene plasmons excited by a swift charged particle with velocity (a) $0.5c$ and (b) $0.7c$. (c) The dependence of the effective semiangle on the velocity of the particle. $\alpha = 19.47$ (degree) is the angle of the caustic boundary at zero velocity limitation. $\alpha = 4.52/v$ (degree) is the asymptote of the effective semiangle at a large particle velocity.

large velocities, which is similar to the recent studies in fluid mechanics [26,27].

In conclusion, we reveal a wave phenomenon of graphene plasmons that is relevant to EELS measurements. We find that graphene plasmons excited by a swift charged particle moving above graphene can form a caustic wave pattern with a semiangle equal to the Kelvin angle, when the velocity of the charged particle is slow. At large velocities, the effective semiangle of the graphene plasmons approaches the Mach angle. These results incorporate the recent development in fluid mechanics into the understanding of graphene plasmon excitation in EELS measurements, and introduce caustic wave theory into the field of graphene plasmonics. The proposed phenomenon might be experimentally verified by placing a scatterer in the vicinity of the electron's trajectory. This scatterer will cast a shadow when the graphene plasmons pass by. Thus, by measuring the angle between the shadow and the trajectory of the electrons, it is possible to demonstrate the proposed phenomenon.

[1] M. Jablan, H. Buljan, and M. Soljačić, Phys. Rev. B **80**, 245435 (2009).

[2] A. Vakil and N. Engheta, Science **332**, 1291 (2011).

[3] J. Chen *et al.*, Nature (London) **487**, 77 (2012).

[4] Z. Fei *et al.*, Nature (London) **487**, 82 (2012).

[5] A. N. Grigorenko, M. Polini, and K. S. Novoselov, Nat. Photonics **6**, 749 (2012).

[6] T. Ando, A. B. Fowler, and F. Stern, Rev. Mod. Phys. **54**, 437 (1982).

[7] T. Eberlein, U. Bangert, R. R. Nair, R. Jones, M. Gass, A. L. Bleloch, K. S. Novoselov, A. Geim, and P. R. Briddon, Phys. Rev. B **77**, 233406 (2008).

[8] M. H. Gass, U. Bangert, A. L. Bleloch, P. Wang, R. R. Nair, and A. K. Geim, Nat. Nanotechnol. **3**, 676 (2008).

[9] Y. Liu, R. F. Willis, K. V. Emtsev, and T. Seyller, Phys. Rev. B **78**, 201403 (2008).

[10] W. Zhou, J. Lee, J. Nanda, S. T. Pantelides, S. J. Pennycook, and J.-C. Idrobo, Nat. Nanotechnol. **7**, 161 (2012).

[11] F. G. De Abajo, Rev. Mod. Phys. **82**, 209 (2010).

[12] C. Powell, Phys. Rev. **175**, 972 (1968).

[13] A. Lucas and M. Šunjić, Phys. Rev. Lett. **26**, 229 (1971).

[14] P. Echenique and J. Pendry, J. Phys. C: Solid State **8**, 2936 (1975).

[15] J. Lecante, Y. Ballu, and D. Newns, Phys. Rev. Lett. **38**, 36 (1977).

[16] R. Garcia-Molina, A. Gras-Marti, A. Howie, and R. Ritchie, J. Phys. C: Solid State **18**, 5335 (1985).

[17] M. Walls and A. Howie, Ultramicroscopy **28**, 40 (1989).

[18] F. J. García de Abajo and P. M. Echenique, Phys. Rev. B **46**, 2663 (1992).

[19] M. I. Bakunov, A. V. Maslov, and S. B. Bodrov, Phys. Rev. B **72**, 195336 (2005).

[20] K. F. Allison, D. Borka, I. Radović, L. Hadžievski, and Z. L. Mišković, Phys. Rev. B **80**, 195405 (2009).

[21] I. Radović, D. Borka, and Z. L. Mišković, Phys. Rev. B **86**, 125442 (2012).

[22] S. Liu, C. Zhang, M. Hu, X. Chen, P. Zhang, S. Gong, T. Zhao, and R. Zhong, Appl. Phys. Lett. **104**, 201104 (2014).

[23] E. H. Hwang and S. Das Sarma, Phys. Rev. B **75**, 205418 (2007).

[24] J. Lighthill, *Waves in Fluids* (Cambridge University Press, New York, 2001).

[25] G. B. Whitham, *Linear and Nonlinear Waves* (Wiley, New York, 1999).

[26] M. Rabaud and F. Moisy, Phys. Rev. Lett. **110**, 214503 (2013).

[27] A. Darmon, M. Benzaquen, and E. Raphaël, J. Fluid Mech. **738**, R3 (2014).

[28] P. Genevet, D. Wintz, A. Ambrosio, A. She, R. Blanchard, and F. Capasso, Nat. Nanotechnol., doi:10.1038/nnano.2015.137 (2015).

[29] Y. A. Kravtsov and Y. I. Orlov, *Caustics, Catastrophes, and Wave Fields*, 2nd ed. (Springer, New York, 1998).

[30] I. Epstein and A. Arie, Phys. Rev. Lett. **112**, 023903 (2014).

[31] V. V. Cheianov, V. Fal'ko, and B. L. Altshuler, Science **315**, 1252 (2007).

[32] J. Cserti, A. Pályi, and C. Péterfalvi, Phys. Rev. Lett. **99**, 246801 (2007).

[33] G. W. Hanson, J. Appl. Phys. **103**, 064302 (2008).

[34] V. P. Gusynin, S. G. Sharapov, and J. P. Carbotte, J. Phys.: Condens. Matter **19**, 026222 (2007).

[35] W. C. Chew, *Waves and Fields in Inhomogeneous Media* (IEEE, New York, 1996).

[36] A. Archambault, T. V. Teperik, F. Marquier, and J. J. Greffet, Phys. Rev. B **79**, 195414 (2009).

[37] See Supplemental Material at http://link.aps.org/supplemental/10.1103/PhysRevB.92.081404 for the derivation of some equations and the animations of the graphene plasmons excited by the particle moving above graphene with different velocities.